Robust entanglement transfer through a disordered qubit ladder

Guilherme M. A. Almeida[a,*], Andre M. C. Souza[b], Francisco A. B. F. de Moura[a], Marcelo L. Lyra[a]

[a] *Instituto de Física, Universidade Federal de Alagoas, 57072-900 Maceió, AL, Brazil*
[b] *Departamento de Física, Universidade Federal de Sergipe, 49100-000 São Cristóvão, SE, Brazil*

Abstract

We study an entanglement transfer protocol in a two-leg ladder spin-1/2 chain in the presence of disorder. In the scenario where the on-site energies and intrachain couplings are correlated, following approximately constant proportions along the chain, we set up a scheme for high-fidelity state transfer via a particular subspace wherein effective fluctuations in the parameters ultimately depend on the degree of such correlations, rather on the disorder featured by each leg individually, accounted by a box distribution of strength W. Moreover, we find that the leakage of information out of that subspace is suppressed upon increasing W and thus the transfer fidelity, evaluated through the entanglement concurrence at the other end of the ladder, also builds up with W.

Keywords: quantum entanglement, quantum communication, correlated disorder, Anderson localization

1. Introduction

In the past decade, 1D spin chains have been regarded as potential quantum communication platforms for a wide variety of tasks (see [1, 2] and references within). In standard quantum-state transfer protocols [3], for instance, the chain must be manufactured in such a way an arbitrary qubit can be faithfully sent from one point to another at some (preferably small) prescribed time following the natural underlying Hamiltonian dynamics of the system.

To do so, a handful of schemes have been put forward since the original proposal in Ref. [3], some relying on fully-engineered couplings [4–6] — thereby yielding perfect transfer through arbitrary distances —, dual-rail encoding [7], strong local magnetic fields [8, 9], and weak end couplings [10–14] to name a few.

Given the possibility of experimental errors in the manufacturing process of the chain and that one is willing not to interfere with the channel while it is operating in order to avoid decoherence and losses, disorder stands out as a major threat to the performance of the protocol. This has motivated several studies on the influence of static fluctuations in the parameters of the chain over the state transfer fidelity [7, 15–30].

It is pretty well established that 1D and 2D single-particle hopping models display Anderson localization for any degree of uncorrelated disorder [31, 32]. A very rich cross-over between localization and delocalization, though, can be found in chains displaying certain kinds of correlated disorder [33–38]. For instance, it was shown in [35] that long-range correlated disorder induces the appearance of a band of extended states with sharp mobility edges thereby indicating a metal-insulator transition. Very recently, we have explored the breakdown of Anderson localization in the context of quantum-state transfer protocols [28–30, 39, 40] and also in a discrete-time quantum walk [41].

Another kind of configuration that deserves attention is quasi-1D models such as ladder networks. In [42], it was reported that a two-leg Aubry-André model displays a metal-insulator transition with multiple mobility edges. They also put forward the possibility of spanning a band of localization-free states coexisting with exponentially-localized modes given the on-site energies and interchain hopping strenghts follow constant proportions along the ladder [43]. de Moura et al. further found out a novel level-spacing statistics associated to it [44]. A generalized version of this wavefunction delocalization engineering for N-leg ladder systems was addressed in [45]. The interplay between channels featuring different degrees and/or types of disorder was investigated in Refs. [46, 47].

Two-leg chains have been very important frameworks

*Corresponding author
Email address: gmaalmeidaphys@gmail.com (Guilherme M. A. Almeida)

for the study of ubiquitous transport properties of DNA molecules [48]. It also deserves notice the fact that some polariton systems — i.e., those involving hybrid light-matter particles, where each component may naturally endure different disorder levels — can be mapped directly onto a single-particle hopping in two coupled chains [49]. Recently, ladder chains have also been explored in the presence of gain and loss, namely in a local $\mathcal{PT}$-symmetric configuration [50].

In this work we bring about the idea of localization-free subspaces spanning over a strongly disordered media with correlated parameters [43, 45] into the context of quantum communication protocols. In particular, we aim to transmit entanglement with high fidelity from one end of a two-leg ladder chain to the other in the presence of disorder. We outline the parameter conditions for which a localization-free channel arises and how to properly encode the initial entangled state in order to send it through. We further consider imperfections in this channel, what leads to localization and leakage of information into the other (much more disordered) subspace. Our main result is that this effect can be avoided when, surprisingly, we *increase* the amount of disorder originally present in the system, while still maintaining the aforementioned correlations. This sort of information backflow induced by Anderson-localization has been addressed in Ref. [51] for a single qubit coupled to a disordered network and so it is paramount to investigate it in the context of quantum communication protocols in engineered qubit chains.

In the following, Sec. 2 we introduce the Hamiltonian model and in Sec. 3 we discuss the conditions for setting up the state transfer channel. In Sec. 4 we display our results for the entanglement transfer performance against disorder and investigate the leakage of information out of the channel. Our conclusions are drawn in Sec. 5.

2. Model and formalism

Here, we deal with a two-leg ladder spin$-1/2$ (qubit) chain of the XX type, with N sites each, described by a Hamiltonian of the form $H = H^{(1)} + H^{(2)} + H_I$, with ($\hbar = 1$)

$$H^{(j)} = \sum_{n=1}^{N} \epsilon_{n,j}\sigma_{n,j}^{+}\sigma_{n,j}^{-} + \sum_{n=1}^{N-1} J_{n,j}(\sigma_{n+1,j}^{+}\sigma_{n,j}^{-} + \text{H.c.}), \tag{1}$$

$$H_I = \sum_{n=1}^{N} \gamma_n(\sigma_{n,2}^{+}\sigma_{n,1}^{-} + \text{H.c.}), \tag{2}$$

where $\sigma_{n,j}^{+}$ ($\sigma_{n,j}^{-}$) raises (lowers) the spin at the n-th site of the j-th chain ($j = 1, 2$), $\epsilon_{n,j}$ stands for the local magnetic field, $J_{n,j}$ is the intrachain exchange parameter, and γ_n is the interchain one. (Note that $\sigma_{n,j}^{+}\sigma_{n,j}^{-}$ differs from $\sigma_{n,j}^{z}$ by a constant.) We assume $J_{n,j}, \gamma_n < 0$ and $J_{n,1} = J_{n,2} \equiv J_n$. Furthermore, we need some coupling scheme to guarantee high fidelity excitation transfer from one end of the chain to the other. Here, in particular, we choose the class of fully-engineered couplings used in perfect state transfer protocols [4], $J_n = J\sqrt{n(N-n)}/(N/2)$, with $n = 1, 2, \ldots, N-1$. Note that the denominator $N/2$ (for even N) has been added so that $\max\{J_n\} = J \equiv 1$ is the energy unit. This scheme induces a linear dispersion relation thereby allowing for transmission of a qubit with maximum fidelity (in an ordered system) in 1D chains with arbitrary size [4]. Experimental realizations of this configuration have been put forward in Refs. [52, 53].

Note that H conserves the total number of excitations and here we are interested in the single-excitation manifold spanned over the ferromagnetic state, that is

$$|\mathbf{n}\rangle^{(j)} = \sigma_{n,j}^{+}\bigotimes_{i=1}^{2}|00\cdots0\rangle^{(i)}, \tag{3}$$

thereby forming a 2N-dimensional Hilbert space [see Fig. 1(a)].

Let us now consider that the on-site potentials $\epsilon_{n,j}$ and the inter-chain coupling rates γ_n are disordered. In particular, let us initially assume they fall within a uniform random distribution in the interval $[-W, W]$, W being the intensity of disorder.

3. Correlated disorder and localization-free subspace

In [43] (see also [44]) it was shown that when $\epsilon_{n,1}$, $\epsilon_{n,2}$, and γ_n obey constant proportions between each other across the chain — say, $\epsilon_{n,2}/\epsilon_{n,1} = \alpha$ and $\gamma_n/\epsilon_{n,1} = \beta$ for all n —, one may perform a local change of basis that decouples the Hamiltonian into two parts. Moreover, it is possible to turn one of these subsystems completely free of fluctuations [43] by setting $\beta^2 = \alpha$. To see this happening, let us define

$$|\mathbf{n}, \pm\rangle = \frac{|\mathbf{n}\rangle^{(1)} \pm |\mathbf{n}\rangle^{(2)}}{\sqrt{2}}, \tag{4}$$

and rewrite Hamiltonian H in terms of these states, to get

$$H = \sum_{\mu=\pm}\Bigg[\sum_{n=1}^{N}\widetilde{\epsilon}_{n,\mu}|\mathbf{n},\mu\rangle\langle\mathbf{n},\mu| + \sum_{n=1}^{N-1}J_n(|\mathbf{n}+\mathbf{1},\mu\rangle\langle\mathbf{n},\mu| + \text{H.c.})\Bigg] + \sum_{n=1}^{N}\widetilde{\gamma}_n(|\mathbf{n},+\rangle\langle\mathbf{n},-| + \text{H.c.}), \tag{5}$$

with

$$\widetilde{\epsilon}_{n,\pm} = \frac{\epsilon_{n,1}+\epsilon_{n,2}}{2} \pm \gamma_n, \tag{6}$$

$$\widetilde{\gamma}_n = \frac{\epsilon_{n,1}-\epsilon_{n,2}}{2}, \tag{7}$$

being the potentials and inter-chain coupling rates, respectively, for the effective ladder with both legs extending over $|\mathbf{n},+\rangle$ and $|\mathbf{n},-\rangle$ [see Fig. 1(b)].

By looking at Hamiltonian (5), we readily note that setting $\epsilon_{n,1} = \epsilon_{n,2}$ leads to the decoupling of both legs as $\widetilde{\gamma}_n = 0$. In addition, when $\epsilon_{n,1} = \gamma_n$ then the anti-symmetric branch takes $\widetilde{\epsilon}_{n,-} = 0$. (Note that those stand for the case $\alpha = \beta = 1$.) The availability of a ordered subspace embedded in a strongly disordered media is very appealing when it comes to running pre-engineered quantum-state transfer protocols. It means that if we have an imperfect (single-leg) chain due to, say, uncorrelated on-site fluctuations, generating another copy of it and coupling them up would lead to a localization-free quantum communication channel as long as the input qubit is properly encoded [e.g. following Eq. (4)], no matter how strong W is.

Now, it is immediate to realize that this second (backup) will not be a *perfect* copy of the original one, what would retain some degree of disorder in the channel and also promote the leakage of information from $|\mathbf{n},-\rangle$ into $|\mathbf{n},+\rangle$ as $\epsilon_{n,1} \neq \epsilon_{n,2}$ and so $\widetilde{\gamma}_n \neq 0$ for all n. Still, even if we allow for small deviations in $\epsilon_{n,2}$ around $\epsilon_{n,1}$, it is possible to keep the channel reasonably safe. For instance, let $\epsilon_{n,2} = \epsilon_{n,1} + \delta_n$, with δ_n being another random number, uniformly distributed within $[-\Delta,\Delta]$ such that $\Delta \ll W$. By looking at Eqs. (6) and (7), we now have $\widetilde{\gamma}_n = -\delta_n/2$ and $\widetilde{\epsilon}_{n,-} = \delta_n/2$. Therefore, the effective disorder in the leg spanned by $\{|\mathbf{n},-\rangle\}$ is solely weighted by Δ and not by W, so that the latter can be made arbitrarily large. Further, as $\Delta \neq 0$ there will be leakage into $\{|\mathbf{n},+\rangle\}$, this subspace now acting as a strongly disordered "environment" with on-site energies given by $\widetilde{\epsilon}_{n,+} = (4\epsilon_{n,1}+\delta_n)/2$ [cf. Fig. 1(b)]. Note

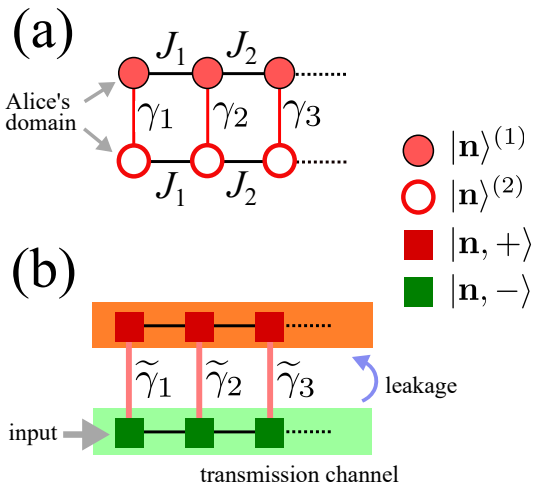

Figure 1: (a) Coupling scheme of the two-leg ladder model described by Eqs. (1) and (2). The on-site potentials ($\epsilon_{n,j}$ with $j = 1,2$) and inter-chain coupling strengths γ_n follow a box-like disorder distribution between $[-W,W]$ each. We set intra-chain couplings to follow $J_n = J\sqrt{n(N-n)}/(N/2)$, with $n = 1,2,\ldots,N-1$. Alice is in charge of the first qubit of each leg and her goal is to prepare an entangled state using hers and sent it to Bob resising at the other end of the ladder. (b) We can also express the ladder Hamiltonian in a more convenient form by changing the basis following Eq. (4). The resulting effective ladder is described by Hamilotonian (5), which feature a localization-free subspace provided $\epsilon_{n,1} = \epsilon_{n,2} = \gamma_n$. If $\epsilon_{n,2}$ deviates a little from $\epsilon_{n,1}$, that is $\epsilon_{n,2} = \epsilon_{n,1} + \delta_n$, with $\delta_n \in [-\Delta,\Delta]$ being another random number, the negative branch (the transmission channel) features some leftover disorder now depending on Δ (not on W). Thus if Alice manages to properly encode her state such that it begins at the first site of such protected channel, the transfer protocol can be relatively shielded from the original disorder strength W although leakage to the positive branch is to take place. Our key result is that this leakage is suppressed as W is increased.

that we are still considering $\gamma_n = \epsilon_{n,1}$. Small deviations from it would not affect $\widetilde{\gamma}_n$, but the on-site potentials $\widetilde{\epsilon}_{n,+}$ and $\widetilde{\epsilon}_{n,-}$. Therefore, here disorder will be ultimately set by W and Δ in the regime $\Delta/W \leq 1$ with $\Delta \ll J$.

4. Results and discussion

4.1. Entanglement transfer

Now, suppose Alice (A) has access to the first cell of the ladder and is willing to send some amount of entanglement to Bob, residing at the other end of the ladder, relying only upon the natural Hamiltonian dynamics of the system [3]. In order to make use of the appropriate ("protected") transmission subspace as discussed in the previous section, a bipartite entangled state of the Bell type can be properly prepared in the form $|\phi\rangle_A = (|10\rangle_A - |01\rangle_A)/\sqrt{2}$. The whole system is then

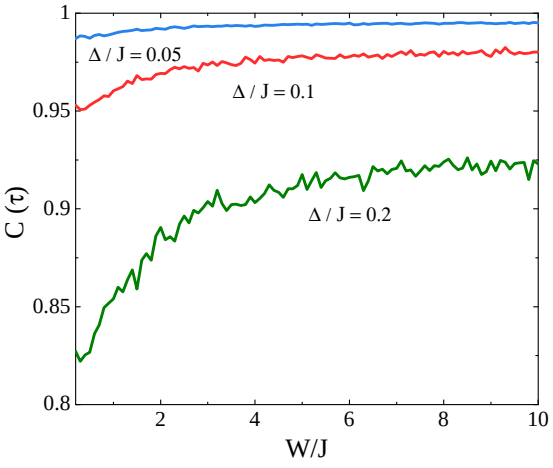

Figure 2: Two-qubit concurrence for the last cell of the ladder system, $C(\tau)$, evaluated at time $\tau = \pi N/(4J)$ against disorder strength W/J (from 0.2 to 10) averaged over 100 distinct realizations. Plots were obtained from exact numerical diagonalization of Hamiltonian (5) for $N = 30$ and $\Delta/J = 0.05, 0.1, 0.2$. The initial state is $|\psi(0)\rangle = |\mathbf{1}, -\rangle$.

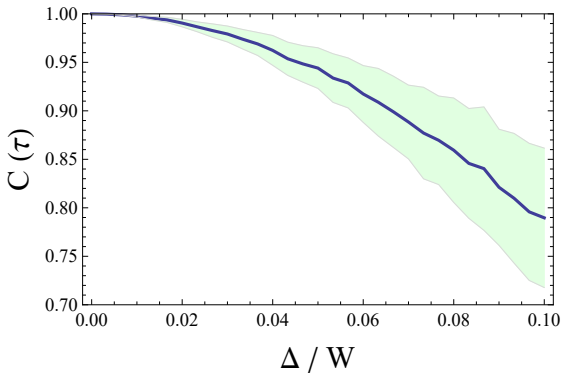

Figure 3: Two-qubit concurrence for the last cell of the ladder system, $C(\tau)$, evaluated at time $\tau = \pi N/(4J)$ against ratio Δ/W averaged over 200 distinct realizations. Green-shaded area is the standard deviation of the mean. Plots were obtained from exact numerical diagonalization of Hamiltonian (5) for $N = 30$ and fixed $W = 3J$. The initial state is $|\psi(0)\rangle = |\mathbf{1}, -\rangle$.

initialized in $|\psi(0)\rangle = |\phi\rangle_A|0\cdots0\rangle^{(1)}|0\cdots0\rangle^{(2)} = |\mathbf{1}, -\rangle$ [cf. Eqs. (3) and 4], which can be thought as a particular case of the dual-rail encoding scheme [7].

We are now to quantify the amount of entangled to reach Bob's cell through unitary evolution of Hamiltonian (5), $U(t) = e^{-iHt}$. For this, we resort to the so-called concurrence [54] which accounts for the entanglement shared between two qubits in any arbitrary mixed state. For single-particle states, all the input we need is the wave function amplitude of both qubits of interest, namely $C(t) = 2|f_N^{(1)}(t)f_N^{(2)}(t)|$, where $f_N^{(j)} = \langle \mathbf{N}^{(j)}|\psi(t)\rangle$ is the transition amplitude to the last site of the j-th leg. For a separable (fully-entangled) state, this quantity reads $C = 0$ ($C = 1$). Note that the transfer performance will be ruled by the likelihood of having $|\psi(\tau)\rangle \approx |\mathbf{N}, -\rangle$ at a given time τ. For the coupling scheme we are using, the transfer time is $\tau = \pi N/(4J)$ [4].

Figure 2 shows the disorder-averaged entanglement concurrence $C(t)$ versus disorder strength W/J evaluated at $t = \tau$ for the encoded initial state $|\psi(0)\rangle = |\mathbf{1}, -\rangle$. There we readily spot a very interesting behavior, namely that the entanglement transfer performance actually gets better upon increasing W. At this point it is convenient to recall that if $\Delta = 0$ then the dynamics takes place on a localization-free subspace, namely an effective ordered 1D chain (see beginning of Sec. 3). In that case, the concurrence would be maximum, $C(\tau) = 1$, entailing a perfect state transfer. In Fig. 2 we see that a local detuning in each cell, $\Delta \neq 0$, lowers the transfer performance. This happens because an effective internal disorder has been induced in branch $\{|\mathbf{n}, -\rangle\}$ whilst some information is leaking from it into $\{|\mathbf{n}, +\rangle\}$. We also mention that these fluctuations affect the transfer time τ. On the other hand, upon increasing W, the concurrence is substantially recovered until saturating. At this regime, the original disorder W no longer has influence on $C(\tau)$. Rather, its saturated (averaged) value is set upon Δ.

The trend seen in Fig. 2 tells us two things: (1) Δ, as it defines the effective diagonal disorder strength in the anti-symmetric branch, also places a limit at the maximum achievable concurrence; (2) this maximum is only reached when W/J is large enough (this is because W prevents leakage of information as will be discussed in the following section). Hence, the ratio Δ/W turns out to be the most appropriate measure of disorder here given the rigorous correlations involved between the parameters and also due to the fact it accounts for how similar is one leg to another ($\Delta/W \ll 1$ means they are quite alike). In Fig. 3 we again evaluate the concurrence at $t = \tau$ but now versus Δ/W, with $W = 3J$. As expected, we loose transfer quality as Δ/W increases but it is possible to keep the entanglement transfer above 90% up to ratios around 6%.

4.2. Leakage dynamics

We now investigate the leakage of information out of the anti-symmetric branch (transmission channel) and the influence of disorder strength W in order to explain the concurrence outcomes seen in Figs. 2 and 3.

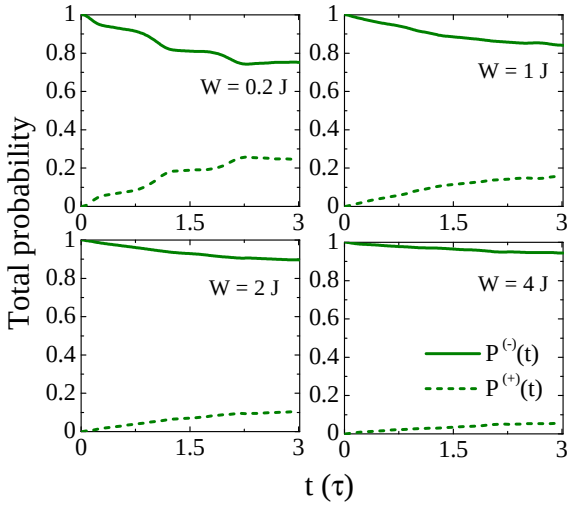

Figure 4: Time evolution of the total occupation probability in the anti-symmetric branch, $P^{(-)}(t) = \sum_n |\langle \mathbf{n}, -|\psi(t)\rangle|^2$ (solid lines), and in the symmetric one, $P^{(+)}(t) = 1 - P^{(-)}(t)$ (dashed lines), for various disorder strengths W, averaged over 100 independent samples. Time is expressed in units of $\tau = \pi N/(4J)$. Plots were obtained from exact numerical diagonalization of Hamiltonian (5) for $N = 30$ and $\Delta/J = 0.2$. Again, the initial state is $|\psi(0)\rangle = |\mathbf{1}, -\rangle$.

Before doing so, we shall get some intuition over the dynamics of disordered ladders by looking at its physical (original) form [Eqs. (1) and (2)]. For a moment, suppose the local energy detuning $\delta_n = \delta$ and $\gamma_n = \gamma$ for all n. If we set an initial state as any linear combination of, say, $\{|\mathbf{n}^{(1)}\rangle\}$, the overall occupation probability to remain in the first leg reads $P^{(1)}(t) = \cos^2(\gamma t)$ for $\delta = 0$ (see Appendix A for details). Thereby, the excitation oscillates back and forth between both legs whereas it propagates following its own intrachain dynamics. For $\delta \neq 0$, $P^{(1)}(t)$ still undergoes periodic oscillations but with smaller amplitude and faster rate (see Eq. (A.7) of Appendix A). The simple picture above tells us in advance that large detunings prevent leakage of information from one leg to the other, as we would have expected intuitively.

Let us now get back to the *effective* ladder chain described by Hamiltonian (5), wherein the local cell detunings and interchain couplings follow a disordered sequence along the array. In Figure 4 we show the time evolution of $P^{(-)}(t) = \sum_n |\langle \mathbf{n}, -|\psi(t)\rangle|^2$ for the same ladder configuration as in Figs. 2 and 3, with initial state $|\psi(0)\rangle = |\mathbf{1}, -\rangle$, averaged over many distinct realizations of disorder. First and foremost, there we clearly see that the disorder strength W indeed prevents the excitation to leak from subspace $\{|\mathbf{n}, -\rangle\}$ into $\{|\mathbf{n}, +\rangle\}$. We shall also mention that the curves look smooth due to the disorder-averaging procedure. Each realization now displays a non-periodic oscillatory behavior. For longer times, the (averaged) total probability reaches about a stationary value which depends on both Δ and W.

We shall get the physical picture underneath the behavior described above by analyzing the on-site energy detuning within each cell. When $\Delta \sim W$ and the system is initialized in the anti-symmetric branch (transmission channel), as the excitation spreads out far away from the initial site it is very likely that it will eventually find some local resonance — a given cell with low detuning $\widetilde{\epsilon}_{n,+} \approx \widetilde{\epsilon}_{n,-}$ — and therefore the excitation is capable of making through the other leg. Chances are extremely low for this to happen upon increasing W and thus the excitation becomes trapped in the original leg for high enough $W \gg \Delta$. What is interesting is that leakage is being prevented while the symmetric (positive) branch is becoming even more disordered (W can be as strong as we wish). Then, as far as the transmission subspace is concerned, what really matters is not the Anderson localization itself taking over the other subspace, but the lack interchain resonances induced by $W \gg \Delta$.

5. Conclusions

We studied an entanglement transfer protocol set over a disordered two-leg ladder qubit chain. By setting up a transmission channel upon demanding certain correlations between the parameters of the ladder while still maintaining the global fluctuations quantified by W, we analyzed the figure of merit of the protocol in the case where those correlations are not perfectly met (accounted by Δ), thus leading to an effective disorder in the channel and promoting the leakage of information out of it. Thus the effective degree of disorder here is ultimately measured by our capability of duplicating a given disordered leg, that is Δ/W as long as $\Delta \ll J$. We showed that the leakage can be suppressed upon increasing W thereby improving the concurrence outcomes at the target location to a great extent. We further explained it by studying the leakage dynamics in detail.

This rather surprising behavior shows us that disorder may be a convenient ingredient to prevent dissipation. Indeed, there has been considerable interest in studying open system dynamics involving structured (such as disordered) environments [51, 55]. In [51], for instance — by looking at the dynamics of a single emitter coupled to an array of cavities acting as the environment — they reported that disorder is able to push information back to the emitter. They further characterized this information backflow using proper non-Markovianity measures. Further extensions of our work may be taken

along this direction. Another possibility is setting up quantum communication protocols in N-leg ladders for which there also exists schemes to induce a localization-free subspace embedded within a strongly-disordered scenario [45].

Experimental realization of our findings should involve single-site addressing in order to adjust the local potential of the second (backup) leg — with the highest possible accuracy so as to assure $\Delta \ll W$ — once the first one is characterized. A potential platform for this could be optical lattices, for which a high degree of single-site resolution has been achieved over the past few years [56–58]. In these systems, the disordered potential can be controlled by an optical speckle field [59, 60]. Anderson localization was also observed in a 2D photonic lattice [61].

The perfect quantum-state transfer scheme [4] has been implemented in an array of 11 coupled waveguides [53]. Technology for fabricating more structured, programmable waveguide lattices is now at reach. In [62], a twodimensional continuous-time quantum walk with single photons has very recentely been realized on a 49×49 grid. This is a considerable step towards the implementation of engineered Hamiltonians with tunable parameters and nontrivial topologies.

Acknowledgments

This work was supported by CNPq, CNPq-Rede Nanobioestruturas, CAPES, FINEP (Federal Brazilian Agencies), and FAPEAL (Alagoas State Agency).

Appendix A. One-leg occupation probability

Here we show how to obtain the overall occupation probability over time in one of the legs of the physical ladder chain [Eq. (A.7)] given $\delta_n = \delta$ and $\gamma_n = \gamma$ for all n [cf. Eqs. (1) and (2)].

Let us denote

$$|\lambda_{k,j}\rangle = \sum_n v_{k,n}^{(j)} |\mathbf{n}\rangle^{(j)}, \tag{A.1}$$

such that it satisfies the eigenvalue equation $H^{(j)}|\lambda_{k,j}\rangle = \lambda_{k,j}|\lambda_{k,j}\rangle$, with $k = 1,\ldots,N$. Now, given $J_{n,1} = J_{n,2}$, both sets of eigenstates ($j = 1, 2$) feature the same spatial profile. Also note that $\lambda_{k,2} = \lambda_{k,1} + \delta$. The interaction Hamiltonian [Eq. (2)] yields $H_I|\lambda_{k,1(2)}\rangle = \gamma|\lambda_{k,2(1)}\rangle$. Thereby we end up with a series of independent dimer-like interactions between the normal modes of each leg. The total Hamiltonian of the system may then be rewritten as $H = \sum_k H_k$, with

$$\begin{aligned} H_k = {} & \lambda_{k,1}|\lambda_{k,1}\rangle\langle\lambda_{k,1}| + \lambda_{k,2}|\lambda_{k,2}\rangle\langle\lambda_{k,2}| \\ & + \gamma(|\lambda_{k,1}\rangle\langle\lambda_{k,2}| + \text{H.c.}). \end{aligned} \tag{A.2}$$

Each dimer can be diagonalized separately and we get

$$|\psi_k^{\pm}\rangle = A^{\pm}|\lambda_{k,1}\rangle + B^{\pm}|\lambda_{k,2}\rangle, \tag{A.3}$$

with

$$A^{\pm} = \frac{2\gamma}{\sqrt{(\delta \pm \Omega)^2 + 4\gamma^2}}, \quad B^{\pm} = \frac{\delta \pm \Omega}{\sqrt{(\delta \pm \Omega)^2 + 4\gamma^2}}, \tag{A.4}$$

and corresponding eigenenergies

$$E_k^{\pm} = \frac{1}{2}(\lambda_{k,1} + \lambda_{k,2} \pm \Omega) = \lambda_{k,1} + \frac{1}{2}(\delta \pm \Omega), \tag{A.5}$$

where $\Omega = \sqrt{\delta^2 + 4\gamma^2}$ is the effective Rabi frequency.

Now, if we initialize the system as a linear combination of the form $|\psi(0)\rangle = \sum_k a_k(0)|\lambda_{k,1}\rangle$, the time-evolved state reads

$$\begin{aligned} |\psi(t)\rangle = U(t)|\psi(0)\rangle &= \sum_{k,\nu=\pm} e^{-iE_k^{\nu}t}|\psi_k^{\nu}\rangle\langle\psi_k^{\nu}|\psi(0)\rangle \\ &= \sum_{\nu=\pm}(A^{\nu})^2 e^{-i\left(\frac{\delta+\nu\Omega}{2}\right)t} \sum_k a_k(t)|\lambda_{k,1}\rangle \\ &\quad + \sum_{\nu=\pm} A^{\nu}B^{\nu} e^{-i\left(\frac{\delta+\nu\Omega}{2}\right)t} \sum_k a_k(t)|\lambda_{k,2}\rangle, \end{aligned} \tag{A.6}$$

where $a_k(t) = a_k(0)e^{-i\lambda_k^{(1)}t}$. Therefore, the wavefunction evolves in time following the intrachain eigenspectrum — which, recall, is the same for both legs — with coefficients $a_k(t)$ modulated by the sums in ν (see equation above). The overall occupation probability $P^{(1)}(t) = \sum_k |\langle\lambda_{k,1}|\psi(t)\rangle|^2$ can then be worked out as

$$P^{(1)}(t) = 1 - 2\left(\frac{\gamma}{\Omega}\right)^2 [1 - \cos(\Omega t)], \tag{A.7}$$

which reduces to $P^{(1)}(t) = \cos^2(\gamma t)$ when $\delta = 0$. Likewise, $P^{(2)} = 1 - P^{(1)}$ for the other leg.

References

[1] T. J. G. Apollaro, S. Lorenzo, F. Plastina, Int. J. Mod. Phys. B 27 (2013) 1345035.

[2] G. M. Nikolopoulos, I. Jex (Eds.), Quantum State Transfer and Network Engineering, Springer-Verlag, Berlin, 2014.

[3] S. Bose, Phys. Rev. Lett. 91 (2003) 207901.

[4] M. Christandl, N. Datta, A. Ekert, A. J. Landahl, Phys. Rev. Lett. 92 (2004) 187902.

[5] M. B. Plenio, J. Hartley, J. Eisert, New Journal of Physics 6 (2004) 36.

[6] G. M. Nikolopoulos, D. Petrosyan, P. Lambropoulos, Europhys. Lett. 65 (2004) 297.
[7] D. Burgarth, S. Bose, New Journal of Physics 7 (2005) 135.
[8] S. Lorenzo, T. J. G. Apollaro, A. Sindona, F. Plastina, Phys. Rev. A 87 (2013) 042313.
[9] S. Lorenzo, T. J. G. Apollaro, S. Paganelli, G. M. Palma, F. Plastina, Phys. Rev. A 91 (2015) 042321.
[10] A. Wójcik, T. Łuczak, P. Kurzyński, A. Grudka, T. Gdala, M. Bednarska, Phys. Rev. A 72 (2005) 034303.
[11] A. Wójcik, T. Łuczak, P. Kurzyński, A. Grudka, T. Gdala, M. Bednarska, Phys. Rev. A 75 (2007) 022330.
[12] Y. Li, T. Shi, B. Chen, Z. Song, C.-P. Sun, Phys. Rev. A 71 (2005) 022301.
[13] G. M. A. Almeida, F. Ciccarello, T. J. G. Apollaro, A. M. C. Souza, Phys. Rev. A 93 (2016) 032310.
[14] G. M. A. Almeida, Phys. Rev. A 98 (2018) 012334.
[15] J. Allcock, N. Linden, Phys. Rev. Lett. 102 (2009) 110501.
[16] G. De Chiara, D. Rossini, S. Montangero, R. Fazio, Phys. Rev. A 72 (2005) 012323.
[17] J. Fitzsimons, J. Twamley, Phys. Rev. A 72 (2005) 050301.
[18] A. Siber, Am. J. Phys. 74 (2006) 692.
[19] D. I. Tsomokos, M. J. Hartmann, S. F. Huelga, M. B. Plenio, New Journal of Physics 9 (2007) 79.
[20] D. Petrosyan, G. M. Nikolopoulos, P. Lambropoulos, Phys. Rev. A 81 (2010) 042307.
[21] N. Y. Yao, L. Jiang, A. V. Gorshkov, Z.-X. Gong, A. Zhai, L.-M. Duan, M. D. Lukin, Phys. Rev. Lett. 106 (2011) 040505.
[22] A. Zwick, G. A. Álvarez, J. Stolze, O. Osenda, Phys. Rev. A 84 (2011) 022311.
[23] A. Zwick, G. A. Álvarez, J. Stolze, O. Osenda, Phys. Rev. A 85 (2012) 012318.
[24] M. Bruderer, K. Franke, S. Ragg, W. Belzig, D. Obreschkow, Phys. Rev. A 85 (2012) 022312.
[25] A. Kay, Phys. Rev. A 93 (2016) 042320.
[26] R. Ronke, M. P. Estarellas, I. D'Amico, T. P. Spiller, T. Miyadera, Eur. Phys. J. D 70 (2016) 189.
[27] M. P. Estarellas, I. D'Amico, T. P. Spiller, Phys. Rev. A 95 (2017) 042335.
[28] G. M. A. Almeida, F. A. B. F. de Moura, T. J. G. Apollaro, M. L. Lyra, Phys. Rev. A 96 (2017) 032315.
[29] G. M. A. Almeida, F. A. B. F. de Moura, M. L. Lyra, Phys. Lett. A 382 (2018) 1335.
[30] G. M. A. Almeida, C. V. C. Mendes, M. L. Lyra, F. A. B. F. de Moura, Annals of Physics 398 (2018) 180.
[31] P. W. Anderson, Phys. Rev. 109 (1958) 1492–1505.
[32] E. Abrahams, P. W. Anderson, D. C. Licciardello, T. V. Ramakrishnan, Phys. Rev. Lett. 42 (1979) 673–676.
[33] D. H. Dunlap, H.-L. Wu, P. W. Phillips, Phys. Rev. Lett. 65 (1990) 88–91.
[34] P. Phillips, H.-L. Wu, Science 252 (1991) 1805–1812.
[35] F. A. B. F. de Moura, M. L. Lyra, Phys. Rev. Lett. 81 (1998) 3735–3738.
[36] F. M. Izrailev, A. A. Krokhin, Phys. Rev. Lett. 82 (1999) 4062–4065.
[37] U. Kuhl, F. M. Izrailev, A. A. Krokhin, H.-J. Stöckmann, Applied Physics Letters 77 (2000) 633–635.
[38] F. Izrailev, A. Krokhin, N. Makarov, Physics Reports 512 (2012) 125 – 254.
[39] G. M. A. Almeida, F. A. B. F. de Moura, M. L. Lyra, Quant. Inf. Proc. 18 (2019) 41.
[40] P. R. S. Junior, G. M. A. Almeida, M. L. Lyra, F. A. B. F. de Moura, Phys. Lett. A (to appear) (2019).
[41] C. V. C. Mendes, G. M. A. Almeida, M. L. Lyra, F. A. B. F. de Moura, Phys. Rev. E 99 (2019) 022117.
[42] S. Sil, S. K. Maiti, A. Chakrabarti, Phys. Rev. Lett. 101 (2008) 076803.
[43] S. Sil, S. K. Maiti, A. Chakrabarti, Phys. Rev. B 78 (2008) 113103.
[44] F. A. B. F. de Moura, R. A. Caetano, M. L. Lyra, Phys. Rev. B 81 (2010) 125104.
[45] A. Rodriguez, A. Chakrabarti, R. A. Römer, Phys. Rev. B 86 (2012) 085119.
[46] W. Zhang, R. Yang, Y. Zhao, S. Duan, P. Zhang, S. E. Ulloa, Phys. Rev. B 81 (2010) 214202.
[47] A.-M. Guo, S.-J. Xiong, Phys. Rev. B 83 (2011) 245108.
[48] R. A. Caetano, P. A. Schulz, Phys. Rev. Lett. 95 (2005) 126601.
[49] H.-Y. Xie, V. E. Kravtsov, M. Müller, Phys. Rev. B 86 (2012) 014205.
[50] B. P. Nguyen, K. Kim, Phys. Rev. A 94 (2016) 062122.
[51] S. Lorenzo, F. Lombardo, F. Ciccarello, G. M. Palma, Scientific Reports 7 (2017) 42729.
[52] M. Bellec, G. M. Nikolopoulos, S. Tzortzakis, Opt. Lett. 37 (2012) 4504–4506.
[53] R. J. Chapman, M. Santandrea, Z. Huang, G. Corrielli, A. Crespi, M.-H. Yung, R. Osellame, A. Peruzzo, Nat. Comm. 7 (2016) 11339.
[54] W. K. Wootters, Phys. Rev. Lett. 80 (1998) 2245–2248.
[55] F. Cosco, M. Borrelli, J. J. Mendoza-Arenas, F. Plastina, D. Jaksch, S. Maniscalco, Phys. Rev. A 97 (2018) 040101.
[56] C. Weitenberg, M. Endres, J. F. Sherson, M. Cheneau, P. Schausz, T. Fukuhara, I. Bloch, S. Kuhr, Nature 471 (2011) 319–324.
[57] T. Fukuhara, A. Kantian, M. Endres, M. Cheneau, P. Schausz, S. Hild, D. Bellem, U. Schollwock, T. Giamarchi, C. Gross, I. Bloch, S. Kuhr, Nat Phys 9 (2013) 235–241.
[58] T. Fukuhara, S. Hild, J. Zeiher, P. Schauß, I. Bloch, M. Endres, C. Gross, Phys. Rev. Lett. 115 (2015) 035302.
[59] J. Billy, V. Josse, Z. Zuo, A. Bernard, B. Hambrecht, P. Lugan, D. Clément, L. Sanchez-Palencia, P. Bouyer, A. Aspect, Nature 453 (2008) 891.
[60] M. Pasienski, D. McKay, M. White, B. DeMarco, Nature Physics 6 (2010) 677.
[61] T. Schwartz, G. Bartal, S. Fishman, M. Segev, Nature 446 (2007) 52.
[62] H. Tang, X.-F. Lin, Z. Feng, J.-Y. Chen, J. Gao, K. Sun, C.-Y. Wang, P.-C. Lai, X.-Y. Xu, Y. Wang, L.-F. Qiao, A.-L. Yang, X.-M. Jin, Science Advances 4 (2018) eaat3174.